Journal of Photochemistry and Photobiology A: Chemistry 205 (2009) 156–160

Contents lists available at ScienceDirect

Journal of Photochemistry and Photobiology A: Chemistry

journal homepage: www.elsevier.com/locate/jphotochem

Highly luminescent di-ureasil hybrid doped with a Eu(III) complex including dipicolinate ligands

Maria E. Mesquita [a,c], S.S. Nobre [b], M. Fernandes [c], R.A.S. Ferreira [b], Sílvia C.G. Santos [a], Marcelo O. Rodrigues [d], L.D. Carlos [b,**], V. de Zea Bermudez [c,*]

[a] Department of Chemistry, UFS, 49100-000 São Cristóvão, SE, Brazil
[b] Department of Physics, CICECO, University of Aveiro, 3810-193 Aveiro, Portugal
[c] Department of Chemistry, CQ-VR, University of Trás-os-Montes e Alto Douro, 5001-801 Vila Real, Portugal
[d] Departamento de Química Fundamental, UFPE, 50590-470 Recife, PE, Brazil

ARTICLE INFO

Article history:
Received 20 December 2008
Received in revised form 27 March 2009
Accepted 27 April 2009
Available online 3 May 2009

Keywords:
Sol–gel
Di-ureasils
Europium dipicolinate complex
Photoluminescence

ABSTRACT

A short chain di-urea cross-linked poly(oxyethylene) (POE)/siloxane hybrid host (di-ureasil), designated as d-U(600), was doped with the $Na_3[Eu(dipic)_s]\cdot xH_2O$ (where $dipic^{2-}$ is the dipicolinate ion) complex. The resulting material is non-porous, semi-crystalline and thermally stable up to 145 °C. Because of the presence of the bulky $dipic^{2-}$ ligands, the addition of the complex to d-U(600) leads to the partial destruction of the hydrogen-bonded POE/urea aggregates of the hybrid matrix and to the formation of extra urea/urea aggregates. The incorporation of the complex into d-U(600) accounts for an increase of both the $^5D_0$ lifetime and quantum efficiency values (1.950 ± 0.007 ms and 0.50, respectively) with respect to those of the isolated complex (1.7 ms and 0.46, respectively). The addition of the complex also contributes to an enhancement of the absolute emission quantum yield value, whose maximum value (0.66 excited at 280 nm) is the highest value reported for organic–inorganic hybrids modified by lanthanide complexes.

1. Introduction

The lanthanide (Ln) ions possess characteristic 4f open-shell configurations, +3 being the most stable oxidation state, and exhibit a close chemical resemblance across the periodic series due to the small and regular decrease in their ionic radii. The Ln^{3+} ions are attractive from the optical standpoint, owing to the shielding of the 4f electrons from interaction with the chemical environment provided by the filled $5s^2$ and $5p^6$ sub-shells. The emission bands, that range from the ultraviolet (UV) to the near infrared (NIR) spectral regions, are *quasi* monochromatic and long-lived. Large pseudo-Stokes shifts are observed and high luminescence quantum yields may be obtained. However, because the parity and spin-forbidden 4f–4f transitions have low molar absorption coefficients that may severely limit the light output, the direct photoexcitation of Ln^{3+} ions is not very efficient.

A significant enhancement of the Ln^{3+} luminescence intensity may be achieved through the design of lanthanide complexes comprising sensitizing ligands, i.e., molecules able to absorb the excitation energy and transfer it to Ln^{3+} ions, which in turn undergo the typical radiative emitting process. This process is known as *antenna* effect [1]. A further advantage of these ligands is that they act as protecting cages, shielding the Ln^{3+} ions from deleterious quenching processes. Such complexes emit in the near-UV (Ce^{3+} and Gd^{3+}), visible (vis) (blue, Tm^{3+}; green, Tb^{3+} and Er^{3+}; yellow, Dy^{3+}; orange, Sm^{3+}; red, Eu^{3+}) and NIR (Nd^{3+}, Er^{3+}, Tm^{3+} and Yb^{3+}) spectral regions and thus are of great interest for a wide range of photonic applications [2]. In these compounds the Ln^{3+} species (hard acids) are strongly bonded to organic molecules bearing adequate donor species (hard bases), typically oxygen and/or nitrogen atoms. Calixarenes, β-diketones, cryptands, podands and heterocyclic and aromatic carboxylic acids have been extensively explored in this context. The pyridinecarboxylate (typically named picolinate (pic^-))-based molecules, which are based on the latter class of ligands, are particularly interesting owing to their chemical stability and photophysical properties [3–5]. These attractive features explain the significant number of systematic studies carried out on lanthanide dipicolinates [4–11]. Complexes formed between Eu^{3+} and pyridine-2,6-dicarboxylic acid (or dipicolinic acid (H_2dipic)) have been proposed for applications in biological systems and immunoassays [12–14].

The incorporation of lanthanide complexes into sol–gel derived organic/inorganic hybrid frameworks [15] represents a suitable strategy that has been adopted in recent years to produce materials with improved luminescence properties [16,17]. A few hybrid

* Corresponding author. Tel.: +351 259 350253; fax: +351 259 350480.
** Co-corresponding author. Tel.: +351 234 370946; fax: +351 234 424695.
E-mail addresses: lcarlos@ua.pt (L.D. Carlos), vbermude@utad.pt (V. de Zea Bermudez).

1010-6030/$ – see front matter © 2009 Elsevier B.V. All rights reserved.
doi:10.1016/j.jphotochem.2009.04.022

materials incorporating lanthanide dipicolinate complexes have been investigated by several authors [18–20].

In the present paper we report for the first time the thermal behaviour, morphology and optical features of a hybrid sample based on a low molecular weight di-urea cross-linked poly(oxyethylene) (POE)/siloxane hybrid matrix (di-ureasil) comprising POE segments with about 8.5 oxyethylene repeat units (designated as d-U(600)) and $Na_3[Eu(dipic)_3]\cdot xH_2O$, a complex in which the Eu^{3+} coordination sphere includes dipicolinate ligands. The properties of di-ureasil structures [21,22] doped with lanthanide ions have been widely explored [23]. So far, the ligands of the few Eu^{3+}-based complexes that have been added to [24–29] or formed within [30] di-ureasil matrices belong to the classes of heterocyclic compounds [24,25,30], β-diketonates [24–29] and phosphine oxides [27].

We will use here an attractive synthesis strategy that we have explored recently in the context of our investigation of the di-ureasils [26,29]. It relies on the addition of lanthanide complexes to these POE/siloxane hybrid networks whose available cation coordinating sites – the carbonyl oxygen atoms of the urea cross-links and/or the ether oxygen atoms of the POE chains – enable *in situ* formation of new complexes devoid of water ligands and improved optical features.

2. Experimental

2.1. Materials

Europium nitrate ($Eu(NO_3)_3\cdot 6H_2O$), pyridine-2,6-dicarboxylic acid (H_2dipic, Aldrich, 99,99%) and 3-isocyanatepropyltriethoxysilane (ICPTES, Fluka) and sodium hydroxide (NaOH, PA Pronalab) were used as received. The O,O′-bis-(2-aminopropyl) polypropylene glycol-block-polyethylene glycol-block-polypropylene glycol employed, commercially designated as Jeffamine ED-600® (Fluka, average molecular weight 600 g mol^{-1}), ethanol (CH_3CH_2OH, Merck, PA grade) and tetrahydrofuran (THF, Merck, puriss. PA grade) were stored over molecular sieves. High purity distilled water was used in all the experiments.

2.2. Synthesis

2.2.1. Synthesis of $Na_3[Eu(dipic)_3]\cdot xH_2O$

The europium dipicolinate complex was prepared according to a procedure reported elsewhere [10].

2.2.2. Synthesis of the di-ureasil samples

A xerogel with a concentration of Eu:Si = 1:146 (g/g) was synthesized using a method described in detail previously [29]. The sample was obtained as a transparent, flexible monolith with an orange-like hue. In agreement with the terminology used in previous papers [22], the hybrid matrix of the material obtained has been designated as d-U(600), where d indicates di, U denotes the urea group and 600 corresponds to the average molecular weight of the starting organic precursors. The doped sample will be henceforth described by the d-U(600)@Eu notation. A non-doped sample (d-U(600)) was also obtained.

2.3. Characterization

The Fourier Transform infrared (FT-IR) spectrum of the doped di-ureasil sample was acquired at room temperature on a Unicam FT-IR spectrophotometer. The spectra were collected in the 4000–500 cm^{-1} range by averaging 120 scans at a resolution of 4 cm^{-1}. About 2 mg of each sample was mixed with potassium bromide (Merck, spectroscopic grade) finely ground and pressed into pellets. The xerogel pellet was kept at 80 °C under vacuum to minimize the levels of absorbed water.

The thermal characteristics of the sample were determined by means of differential scanning calorimetry (DSC) and thermogravimetric analysis (TGA). For the DSC experiment a disk section of the xerogel with a mass of approximately 10 mg was placed in a 30 μl aluminium can and stored in a desiccator over phosphorous pentoxide (P_2O_5) for 1 week at room temperature under vacuum. After this drying treatment the can was hermetically sealed and the thermogram was recorded using a DSC131 Setaram differential scanning calorimeter. The sample was heated at 10 °C min^{-1} from 25 to 190 °C. For the TGA experiments the xerogel was first stored in a desiccator over P_2O_5. It was subsequently transferred to an open platinum crucible and analyzed from 25 to 800 °C using a TA Instruments Q50 thermobalance at a heating rate of 10 °C min^{-1}. In both experiments the purge gas used was high purity nitrogen supplied at a constant 30 (DSC)/20 (TGA) cm^3 min^{-1} flow rate.

To evaluate the morphology of the xerogel film, scanning electronic microscopy (SEM) micrographs were obtained using a SEM/ESEM-FEI Quanta 400 scanning electron microscope at high acceleration voltage (20 kV). A small portion of the sample was cut, fixed on an aluminium stub with carbon tape and then coated with Au/Pd.

X-ray diffraction (XRD) measurements were performed at room temperature with a PANalytical X'Pert Pro equipped with a X'Celerator detector using monochromated CuK_α radiation (λ = 1.541 Å) over the 2θ range between 10° and 70°. The xerogel sample, analyzed as a film, was not submitted to any thermal pretreatment.

The photoluminescence features were recorded at room temperature with a modular double grating excitation spectrofluorimeter with a TRIAX 320 emission monochromator (Fluorolog-3, Jobin Yvon-Spex) coupled to a R928 Hamamatsu photomultiplier, using the front face acquisition mode. The excitation source was a 450 W Xe arc lamp. The emission spectra were corrected for detection and optical spectral response of the spectrofluorimeter and the excitation spectra were weighted for the spectral distribution of the lamp intensity using a photodiode reference detector. The lifetime measurements were acquired with the setup described for the luminescence spectra using a pulsed Xe–Hg lamp (6 μs pulse at half width and 20–30 μs tail).

The absolute emission quantum yields were measured at room temperature using a quantum yield measurement system C9920-02 from Hamamatsu with a 150 W Xe lamp coupled to a monochromator for wavelength discrimination, an integrating sphere as sample chamber and a multichannel analyzer for signal detection. Three measurements were made for each sample so that the average value is reported. The method is accurate to within 10%.

3. Results and discussion

In an attempt to elucidate the role played by the complex on the hydrogen-bonded array of d-U(600) we inspected the "amide I" region of the non-doped and doped xerogels. Classical deconvolution techniques of the 1750–1600 cm^{-1} interval [31] allowed us to resolve the "amide I" band profile of d-U(600) and d-U(600)@Eu hybrid into five and four components, respectively (Fig. 1). The spectral data indicate that the addition of an extremely small amount of $Na_3[Eu(dipic)_3]\cdot xH_2O$ to d-U(600) affects the global profile of the "amide I" band. The intensity maximum of the "amide I" envelope is shifted from approximately 1653 to 1645 cm^{-1}, a proof that the hydrogen bonds in the doped sample are globally stronger than those in the non-doped host matrix. Doping results in considerable band redistribution, meaning that the proportion of hydrogen-bonded aggregates in the material suffers marked changes. Upon

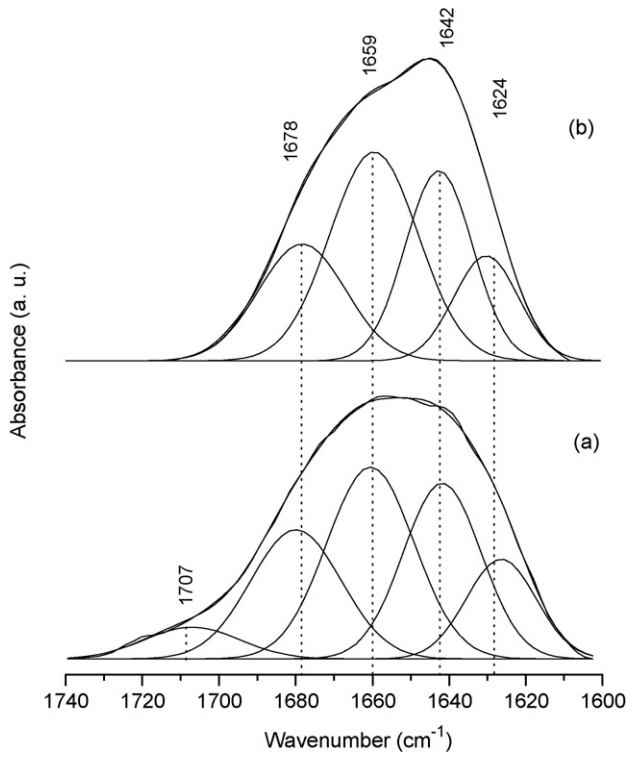

Fig. 1. Curve fitting results of the FT-IR spectra of d-U(600) (a) and d-U(600)@Eu (b).

incorporation of $Na_3[Eu(dipic)_3]{\cdot}xH_2O$ into the d-U(600) framework the 1707 cm^{-1} band (Fig. 1(a)), attributed to the presence of weak hydrogen-bonded POE/urea aggregates [22,32–34] vanishes (Fig. 1(b)), revealing that the most disordered hydrogen-bonded aggregates of d-U(600) are completely destroyed. Concomitantly the amount of stronger aggregates increases. The absence of a band at 1750 cm^{-1} band in the "amide I" region of the doped material (Fig. 1(b)), associated with urea groups free from any interaction [22,32–34], suggests that all the cross-links of the d-U(600)@Eu sample are involved in hydrogen bonding interactions, similarly to the situation observed in the non-doped matrix. Given the extremely low concentration of the complex in the doped sample examined (*cf.* Section 2.2) and considering the bulkiness of the $dipic^{2-}$ ligand, we may venture that the rupture of the hydrogen bonds observed appears to be solely a consequence of the existence of severe steric constraints [35,36]. Thus, one of the most critical points that will remain unconfirmed in the present work is the coordination of the Eu^{3+} ions to the urea carbonyl groups in the europium complex. In lanthanide complex-doped di-ureasils the coordination of the lanthanide ions to the carbonyl oxygen atoms of the urea cross-links of the hybrid matrix may be easily monitored in the "amide I" region through the detection of a new event that emerges typically around 1620 cm^{-1} [24,25]. In the "amide I" region of d-U(600)@Eu this Eu^{3+} coordination-sensitive feature is not detected (Fig. 1(b)). It is very likely, however, that the concentration of Eu^{3+} is too low to yield a detectable band by FT-IR.

The XRD patterns of the d-U(600)@Eu hybrid are reproduced in Fig. 2. The diffractogram of the hybrid displays the characteristic broad, Gaussian band centred around 21°, associated with ordering within the siliceous domains [37]. In addition, several Bragg peaks are distinctly seen in this diffractogram. As these peaks do not correspond to those of the free complex (not shown), the nature of the new crystalline phase formed in the hybrid medium will remain unknown.

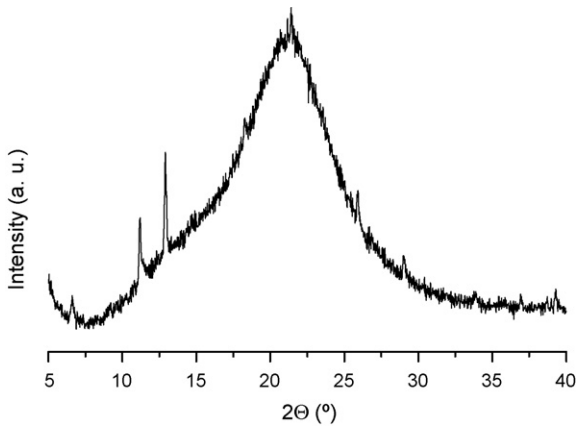

Fig. 2. XRD patterns of the $Na_3[Eu(dipic)_3]{\cdot}xH_2O$ complex (a) and of the d-U(600)@Eu hybrid (b).

The DSC curve of the d-U(600)@Eu hybrid material (not shown) reveals that this sample is entirely amorphous within the range of temperatures examined. On the basis of the conclusions drawn from the XRD data, we may deduce that the new crystalline phase formed within the amorphous hybrid d-U(600) structure upon addition of the complex has a melting temperature higher than the maximum temperature examined by DSC. The d-U(600)@Eu hybrid starts to decompose at about 145 °C (Fig. 3). The thermal degradation takes place in only two stages.

The SEM micrograph reproduced in Fig. 4 demonstrates that the doped hybrid sample displays a non-porous texture. The morphology of this sample is composed of a homogeneous, smooth surface of the hybrid host material in which complex-containing spherical particles with an average diameter of 1.34–0.67 μm are uniformly dispersed, as confirmed by an EDX probe. This type of morphology is similar to that reported very recently for dextrin microparticles incorporating $[Eu(dipic)_3]^{3-}$ ions [38].

The excitation spectrum of the d-U(600)@Eu was monitored within the $^5D_0 \rightarrow {}^7F_2$ transition (Fig. 5). This spectrum displays a large broad band ascribed to the overlap between the $\pi \rightarrow \pi^*$ transitions of the organic ligands [9] with the hybrid host excited states as we will discuss next. Fig. 5 also shows the typical excitation spectrum monitored within the hybrid host intrinsic emission, which is formed of a broad band between 280 and 450 nm, attributed to donor–acceptor pairs recombination occurring in the siliceous and urea-cross-linkages, respectively [37–42]. The overlap between the hybrids' broad band and the excitation spectrum monitored within the Eu^{3+} emission lines (Fig. 5) indicates the existence of hybrid-to-

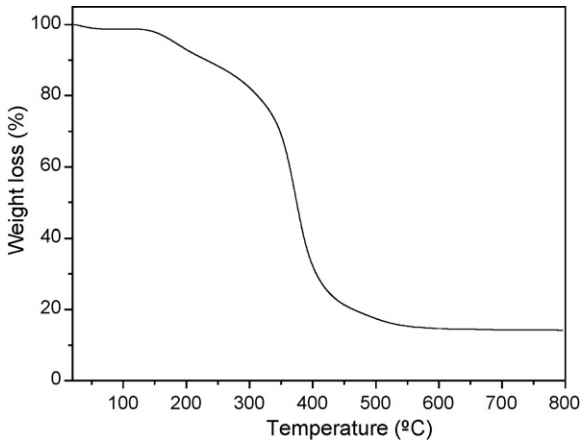

Fig. 3. TGA curve of the d-U(600)@Eu hybrid.

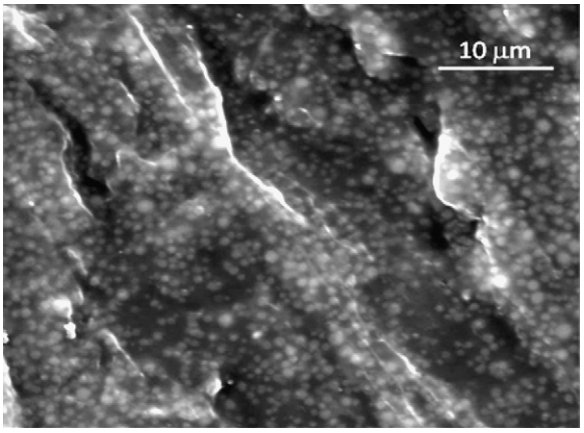

Fig. 4. SEM image of the d-U(600)@Eu hybrid.

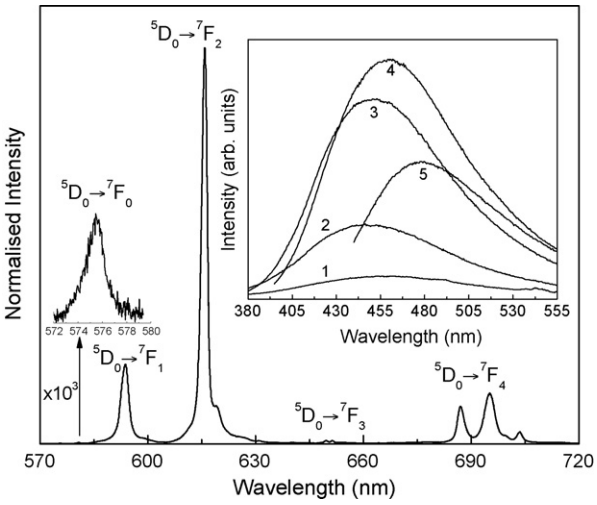

Fig. 6. Emission spectrum of the d-U(600)@Eu hybrid excited at 280 nm. The inset shows the emission spectra excited at (1) 280 nm, (2) 330 nm, (3) 360 nm, (4) 380 nm, and (5) 420 nm.

Eu^{3+} energy transfer. The negligible intensity of the Eu^{3+} intra-4f^6 lines in the excitation spectrum monitored within the Eu^{3+} emission lines (Fig. 5) points out that the Eu^{3+} sensitization process is more efficient than direct excitation into the 4f lines.

Fig. 6 displays the Eu^{3+} emission features of the d-U(600)@Eu hybrid under UV excitation. The spectrum shows a series of lines ascribed to the $^5D_0 \rightarrow {}^7F_{0-4}$ transitions and a low-relative intensity broad band whose peak position deviates to the red as the excitation wavelength increases (280–420 nm) (inset in Fig. 6). Such broad band was already detected for the non-doped d-(600) di-ureasil [37,39–42], and other analogous hybrids, such as the di-urethanesils [25,39] and the mono- [43] and di-amidosils [44]. Its origin has been ascribed to the overlap of two distinct emissions mediated by donor–acceptor pair transitions that occur within the urea, urethane or amide, respectively, cross-linkages and within the siliceous skeleton, due to the presence of oxygen related defects, $^{\bullet}O{-}O{-}Si{\equiv}(CO_2)$ [37–42].

The experimental values for the intensity parameters (Ω_2, Ω_4) for the hybrid were determined from the emission spectrum following a methodology detailed elsewhere [24,27,45]. The obtained values for Ω_2 and Ω_4 are 5.80×10^{-20} and 1.48×10^{-20} cm^2, respectively. The values obtained for Ω_2 suggest that Eu^{3+} is in a less polarisable chemical environment when compared with efficient systems including β-diketonate ligands [24,27,45,46]. The value of Ω_2 for the hybrid reflects, not only the hypersensitive behaviour of the $^5D_0 \rightarrow {}^7F_2$ transition, but also that it is in a low polarisable chemical environment in comparison to the situation found in the complex, which displays a higher Ω_2 value (6.125×10^{-20} cm^2) [9].

The $^5D_0$ emission decay curve was monitored within the $^5D_0 \rightarrow {}^7F_4$ transition excited at 280 nm (Fig. 7). For time values below 1.00 ms the emission decay curve displays a rise time behaviour (inset in Fig. 7) followed by a single exponential function characterized by a lifetime value of 1.950 ± 0.007 ms. This value is higher than that found for the isolated complex, suggesting an effective interaction between the hybrid host and the complex. The higher value found for the hybrid material relatively to that of the isolated complex (1.7 ms) [9] may be further interpreted through the estimation of the $^5D_0$ radiative (A_r) and non-radiative (A_{nr}) transition probabilities, and the quantum efficiency (q) [$q = A_r/A_r + A_{nr}$] based on the emission spectrum and $^5D_0$ lifetime ($\tau^{-1} = A_r + A_{nr}$) [17]. The radiative contribution is calculated from the relative intensities of the $^5D_0 \rightarrow {}^7F_{0-4}$ transitions (the $^5D_0 \rightarrow {}^7F_{5,6}$ branching ratios are neglected due to their poor relative intensity with respect to that of the remaining $^5D_0 \rightarrow {}^7F_{0-4}$ lines). The $^5D_0 \rightarrow {}^7F_1$ transition does not depend on the local ligand field and thus may be used as a reference for the whole spectrum. An effective refractive index of 1.5 was used leading to $A_{01} \approx 50\ s^{-1}$, where A_{01} stands for the Einstein's coefficient of spontaneous emission between the $^5D_0$ and the $^7F_1$ Stark levels. The estimated values for A_r, A_{nr} and q are 0.256 ms^{-1},

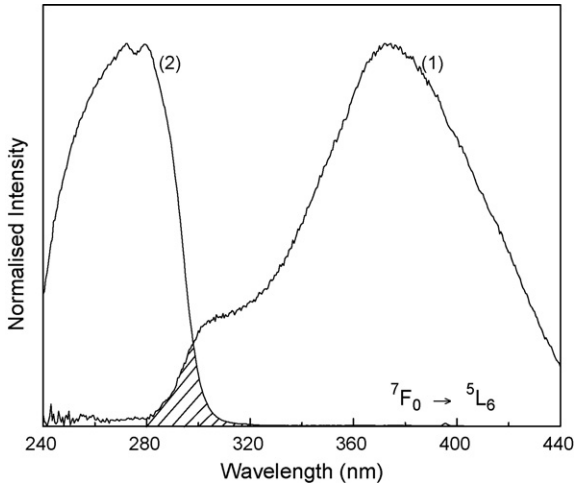

Fig. 5. Excitation spectra of the d-U(600)@Eu hybrid monitored at (1) 460 nm and (2) 615.0 nm. The shadow region assigns the overlap between the two spectra.

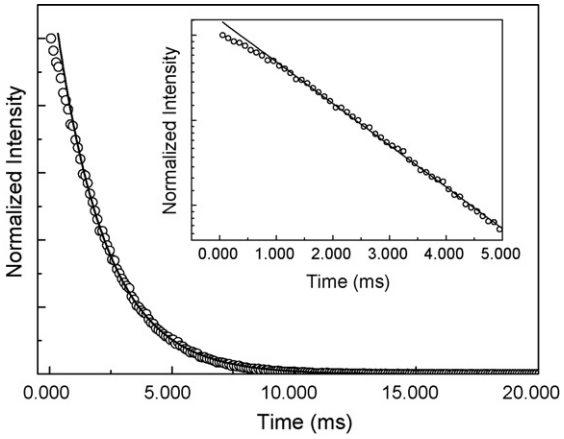

Fig. 7. Emission decay curve of the d-U(600)@Eu hybrid excited at 280 nm and monitored at 615 nm. The solid line corresponds to the data best fit using a single exponential function ($R > 0.99$). The inset shows a magnification of the emission decay curve in the time interval 0.00–5.00 ms plotted in semi-log scale.

$0.256\,ms^{-1}$ and 0.50, respectively. Comparing these values with those previously reported for the isolated complex ($A_r = 0.276\,ms^{-1}$, $A_{nr} = 0.312\,ms^{-1}$ and $q = 0.46$) [9] we may conclude that the complex incorporation into the d-U(600) host leads to an increase in the q value, essentially, due to an increase in the A_r value.

The absolute emission quantum yield (ϕ) for the d-U(600)@Eu hybrid was measured under 280 and 370 nm excitation wavelengths being 0.66 and 0.15, respectively. Both values are higher that the quantum yield known for the isolated complex (0.06 excited at 370 nm) [9], reinforcing that its incorporation into the hybrid network enhances the overall emission features. In particular, we should give emphasis that the increase of the measured absolute emission quantum yield values for the hybrid, when compared with the values obtained for the isolated complex, may be attributed to the effective interaction between the hybrid host and the complex [26,29] and to the contribution of the hybrids' intrinsic emission to the overall photoluminescence features (Fig. 6). Moreover, we stress the maximum quantum yield value (0.66 under 280 nm excitation wavelength) is the highest value reported for organic–inorganic hybrids modified by lanthanide complexes [17]. We should note that, although by definition $q \geq \phi$, the observation of a lower q value (0.50) relatively to the ϕ value (0.66) under the same excitation wavelength (280 nm) results from the contribution of the hybrids' intrinsic emission to the overall luminescence features.

4. Conclusion

A europium dipicolinate complex was added to the short chain d-U(600) di-ureasil POE/siloxane hybrid structure prepared by the sol–gel method. The addition of the $Na_3[Eu(dipic)_3]{\cdot}xH_2O$ complex to d-U(600) has major consequences in terms of hydrogen bonding interactions, leading to a significant breakdown of the most disordered hydrogen-bonded aggregates of d-U(600) and to the concomitant formation of stronger aggregates. This effect was associated with the bulkiness of the ligands. The hybrid sample is thermally stable up to 145 °C and has a non-porous texture, being composed of a homogeneous, smooth surface of the hybrid host material and 1.34–0.67 μm-diameter spherical particles of complex. In spite of the low complex concentration, a crystalline phase of unknown nature is formed in the doped xerogel. Upon incorporation of $Na_3[Eu(dipic)_3]{\cdot}xH_2O$ into the di-ureasil matrix, an increase of both the $^5D_0$ lifetime and quantum efficiency values (1.950 ± 0.007 ms and 0.50, respectively) with respect to those of the isolated complex (1.7 ms and 0.46, respectively) results. The complex incorporation also contributes to enhance the absolute emission quantum yield value, whose maximum value (0.66 excited at 280 nm) is the highest value reported so far for lanthanide-containing organic–inorganic hybrids. This quantum yield enhancement can be attributed to the effective interaction occurring between the hybrid host and the complex and to the contribution of the hybrids' intrinsic emission to the overall photoluminescence features.

Acknowledgements

The financial support from CAPES and CNpq (Brazilian agencies) is gratefully acknowledged. S. Nobre and M. Fernandes thank Fundação para a Ciência e a Tecnologia (Portuguese Agency) for grants (SFRH/BD/28739/06 and SFRH/BD/38530/07, respectively).

References

[1] J.M. Lehn, Angew. Chem. Int. Ed. 29 (1990) 1304.
[2] J.-C. Bünzli, C. Piguet, Chem. Soc. Rev. 34 (2005) 1048.
[3] C. Qin, X.L. Wang, E.B. Wang, Z.M. Su, Inorg. Chem. 44 (2005) 7122.
[4] J.B. Lamture, Z. Hong Zhou, A. Suresh Kumar, T.G. Wensel, Inorg. Chem. 34 (1995) 864.
[5] M.E. de Mesquita, S.A. Júnior, F.C. Oliveira, R.O. Freire, N.B.C. Júnior, G.F. De Sá, Inorg. Chem. Commun. 5 (2002) 292.
[6] A. Fernandes, J. Jaud, J. Dexpert-Ghys, C. Brouca-Cabarrecq, Polyhedron 20 (2001) 2385.
[7] A.-L. Gassner, C. Duhot, J.-C.G. Bünzli, A.-S. Chauvin, Inorg. Chem. 47 (2008) 7802.
[8] M.O. Rodrigues, N.B. da Costa Júnior, C.A. de Simone, A.A.S. Araújo, A.M. Brito-Silva, F.A. Almeida Paz, M.E. de Mesquita, S.A. Júnior, R.O. Freire, J. Phys. Chem. B 112 (2008) 4204.
[9] P.P. Lima, O.L. Malta, S. Alves Júnior, Quim. Nova 28 (2005) 805.
[10] N. Tancrez, C. Feuvrie, I. Ledoux, J.Z. Yss, L. Toupet, H. Le Bozec, O. Maury, J. Am. Chem. Soc. 127 (2005) 13474.
[11] C. Reinhard, H.U. Guldel, Inorg. Chem. 41 (2002) 1048.
[12] A. D'Aléo, A. Picot, A. Beeby, J.A. Gareth Williams, B. Le Guennic, C. Andraud, O. Maury, Inorg. Chem. 47 (2008) 10258.
[13] M.L. Cable, J.P. Kirby, K. Sorasaenee, H.B. Gray, A. Ponce, J. Am. Chem. Soc. 129 (2007) 1474.
[14] A. D'Aléo, G. Pompidor, B. Elena, J. Vicat, P.L. Baldeck, L. Toupet, R. Kahn, C. Andraud, O. Maury, Chem. Phys. Chem. 8 (2007) 2125.
[15] P. Gomez-Romero, C. Sanchez, Functional Hybrid Materials, Wiley Interscience, New York, 2003.
[16] L.D. Carlos, R.A. Sá Ferreira, V. de Zea Bermudez, in: G. Kickelbick (Ed.), Hybrid Materials—Synthesis, Characterization and Applications, Wiley–VCH Verlag GmbH & Co. KGaA, Weinheim, 2007, Cp. 9.
[17] L.D. Carlos, R.A. Sá Ferreira, V. de Zea Bermudez, S.J.L. Ribeiro, Adv. Mater. 21 (2009) 509.
[18] A.C. Franville, D. Zambon, R. Mahiou, Y. Troin, Chem. Mater. 12 (2000) 428.
[19] K. Driesen, R. Van Deun, C. Gorller-Walrand, K. Binnemans, Chem. Mater. 16 (2004) 1531.
[20] K. Lunstroot, K. Driesen, P. Nockemann, K. Van Hecke, L. Van Meervelt, C. Gorller-Walrand, K. Binnemans, S. Bellayer, L. Viau, J. Le Bideau, A. Vioux, Dalton Trans. (2009) 298.
[21] M. Armand, C. Poinsignon, J.-Y. Sanchez, V. de Zea Bermudez, US Patent 5,283,310 (1993).
[22] V. de Zea Bermudez, L.D. Carlos, L. Alcácer, Chem. Mater. 11 (1999) 569.
[23] R.A. Sá Ferreira, L.D. Carlos, V. de Zea Bermudez, in: H.S. Nalwa (Ed.), Encyclopedia of Nanoscience and Nanotechnology, American Scientific Publishers, North Lewis Way, CA, USA, 2004, Cp. 4.
[24] P.P. Lima, R.A. Sá Ferreira, R.O. Freire, F.A. Paz, L. Fu, L.S. Alves Júnior, L.D. Carlos, O.L. Malta, Chem. Phys. Chem. 7 (2006) 735.
[25] L. Fu, R.A. Sá Ferreira, N.J.O. Silva, A.J. Fernandes, P. Ribeiro-Claro, I.S. Gonçalves, V. de Zea Bermudez, L.D. Carlos, J. Mater. Chem. 15 (2005) 3117.
[26] C. Molina, K. Dahmouche, Y. Messadeq, S.J.L. Ribeiro, M.A.P. Silva, V. de Zea Bermudez, L.D. Carlos, J. Lumin. 93 (2003) 104.
[27] P.P. Lima, S.A. Junior, O.L. Malta, L.D. Carlos, R.A. Sá Ferreira, R. Pavithran, M.L.P. Reddy, Eur. J. Inorg. Chem. 19 (2006) 3923.
[28] P.P. Lima, R.A.S. Ferreira, S.A. Júnior, O.L. Malta, L.D. Carlos, J. Photochem. Photobiol. A 201 (2009) 214.
[29] M. Fernandes, V. de Zea Bermudez, R.A. Sá Ferreira, L.D. Carlos, N.V. Martins, J. Lumin. 128/2 (2007) 205.
[30] L. Fu, R.A. Sá Ferreira, S.S. Nobre, L.D. Carlos, J. Rocha, J. Lumin. 122–123 (2006) 265.
[31] PeakFit®, Jandel Scientific, Peak separation and analysis software for Windows, San Rafael, CA, 1995.
[32] V. de Zea Bermudez, R.A. Sá Ferreira, L.D. Carlos, C. Molina, K. Dahmouche, S.J.L. Ribeiro, J. Phys. Chem. B 105 (2001) 3378.
[33] S.C. Nunes, V. de Zea Bermudez, D. Ostrovskii, L.D. Carlos, J. Mol. Struct. 702 (2004) 39.
[34] L. Fu, R.A. Sá Ferreira, M. Fernandes, S.C. Nunes, V. de Zea Bermudez, G. Hungerford, L.D. Carlos, Opt. Mater. 30 (2008) 1058.
[35] M. Fernandes, V. de Zea Bermudez, R.A. Sá Ferreira, L.D. Carlos, A. Charas, J. Morgado, M.M. Silva, M.J. Smith, Chem. Mater. 19 (2007) 3892.
[36] M. Fernandes, S.S. Nobre, M.C. Gonçalves, A. Charas, J. Morgado, R.A.S. Ferreira, L.D. Carlos, V. de Zea Bermudez, J. Mater. Chem. 19 (2009) 733.
[37] L.D. Carlos, V. de Zea Bermudez, R.A. Sá Ferreira, L. Marques, M. Assunção, Chem. Mater. 11 (3) (1999) 581.
[38] P.P. Luz, A.M. Pires, O.A. Serra, J. Fluoresc. 18 (2008) 695.
[39] L.S. Fu, R.A.S. Ferreira, N.J.O. Silva, L.D. Carlos, V. de Zea Bermudez, J. Rocha, Chem. Mater. 16 (2004) 1507.
[40] L.D. Carlos, R.A.S. Ferreira, R.N. Pereira, M. Assuncão, V. de Zea Bermudez, J. Phys. Chem. B 108 (2004) 14924.
[41] S.S. Nobre, P.P. Lima, L. Mafra, R.A. Sá Ferreira, R.O. Freire, L. Fu, U. Pischel, V. de Zea Bermudez, O.L. Malta, L.D. Carlos, J. Phys. Chem. C 111 (2007) 3275.
[42] L.D. Carlos, R.A.S. Ferreira, V. de Zea Bermudez, S.J.L. Ribeiro, Adv. Funct. Mater. 11 (2001) 111.
[43] L.D. Carlos, V. de Zea Bermudez, V.S. Amaral, S.C. Nunes, N.J.O. Silva, R.A.S. Ferreira, J. Rocha, C.V. Santilli, D. Ostrovskii, Adv. Mater. 19 (2007) 341.
[44] S.C. Nunes, V.D.Z. Bermudez, J. Cybinska, R.A.S. Ferreira, J. Legendziewicz, L.D. Carlos, M.M. Silva, M.J. Smith, D. Ostrovskii, J. Rocha, J. Mater. Chem. 15 (2005) 3876.
[45] L.D. Carlos, Y. Messaddeq, H.F. Brito, R.A.S. Ferreira, V. de Zea Bermudez, S.J.L. Ribeiro, Adv. Mater. 12 (2000) 594.
[46] O.L. Malta, H.F. Brito, J.F. Menezes, F.R.G. Silva, S. Alves Jr., S.F. Farias Jr., A.V.M. de Andrade, J. Lumin. 75 (1997) 255.